Dispersion of Nanoclay into Polypropylene with Carbon Dioxide in the Presence of Maleated Polypropylene

Quang T. Nguyen, Donald G. Baird

Department of Chemical Engineering, Virginia Polytechnic Institute and State University, Blacksburg, Virginia 24061-0211

Received 4 June 2007; accepted 28 January 2008
DOI 10.1002/app.28081
Published online 11 April 2008 in Wiley InterScience (www.interscience.wiley.com).

ABSTRACT: The effect of maleic anhydride grafted polypropylene (PP-*g*-MA) on the mechanical and rheological properties of polypropylene (PP)–clay nanocomposites prepared with nanoclay expanded with CO_2 and direct melt blending was studied. The results from the studies of the mechanical properties, rheological properties, and transmission electron microscopy show that when PP-*g*-MA was combined with the technique that used CO_2, greater enhancements in the mechanical properties and degree of dispersion of nanoclay in PP were observed. Furthermore, yieldlike behavior in the viscosity and a tail in the low-frequency behavior of the elastic modulus was attributed to the reaction of PP-*g*-MA with the nanoclay surface and not exfoliation. A fairly well-dispersed morphology was observed for concentrations as high 6.8 wt % clay when the clay was expanded and mixed with CO_2. At this concentration, mechanical properties such as yield strength and modulus increased by as much as 13 and 69%, respectively, relative to the pure PP. Furthermore, the modulus of the composite samples prepared with PP-*g*-MA and CO_2 was some 15% higher than that of samples prepared by direct melt compounding (without the use of CO_2). © 2008 Wiley Periodicals, Inc. J Appl Polym Sci 109: 1048–1056, 2008

Key words: extrusion; organoclay; nanocomposites

INTRODUCTION

Much academic and industrial research in polymer layered-silicate nanocomposites has been rapidly increasing at an unprecedented level because of the potential of these compounds for enhanced physical, chemical, and mechanical properties compared to conventionally filled composites.[1–6] It is well established that when layered silicates are uniformly dispersed and exfoliated in a polymer matrix, the polymer properties can be improved by a dramatic extent. These improvements may include increased strength;[7] higher modulus,[8–13] thermal stability,[14–16] and barrier properties;[17,18] and decreased flammability.[19–23]

The main reason for these marked improvements stem from the large aspect ratio of layered silicate, for example, montmorillonite (MMT). Each individual layer of MMT has a thickness on the order of 1 nm with lengths ranging from 100 to 300 nm.[24,25] The high aspect ratio leads to a high contact surface area and, thus, physical interactions between the polymer and layered silicates with only a small concentration of clay. However, because the layered silicates typically exist as aggregates due to attractive van der Waals forces,[26] the contact surface area available and, thus, improvements in physical properties do not reach theoretical expectations. Achieving a nanocomposite with an exfoliated morphology in which each individual layered silicate has been separated from its initial stack and dispersed uniformly throughout a given polymer matrix is the key to reaching the full potential of the nanoclays to enhance the mechanical, thermal, and barrier properties of a polymeric matrix.

The attractive interactions between the polymer matrix and the layered silicates determine, in large part, the degree of compatibility between the two separate phases. Layered silicates are naturally hydrophilic, whereas many polymers, such as polyolefins, are hydrophobic, and thus, the surface energies between the two materials can be vastly different, which prohibits any significant degree of dispersion of nanoclay within the polymer.[11] To successful develop clay-based nanocomposites, it is necessary to chemically modify a natural clay so that it can be compatible with a chosen polymer matrix. The modification of layered silicates via ion-exchange reactions through which quaternary alkyl ammonium cations replace the existing cations (e.g., Na^+, Ca^+,

Correspondence to: Q. T. Nguyen (qnguyen@vt.edu).
Contract grant sponsor: Environmental Protection Agency; contract grant number: R-82955501-0.
Contract grant sponsor: National Science Foundation; contract grant number: CTS-0507995.

Li^+) residing in the interlayer of the silicates help to make the layered silicates more organophilic. Generally, this can be done through ion-exchange reactions by the replacement of the interlayer cations with quaternary alkylammonium or alkylphosphonium cations.[27–29]

For polymers containing polar functional groups, an alkylammonium surfactant is adequate to promote nanocomposite formation. For nonpolar polypropylene (PP), however, it is not simple because interfacial bonding between the clay surface and PP matrix is unfavorable. To increase the compatibility between MMT nanoclays and PP matrix, two major methods, including melt intercalation[30–35] and *in situ* polymerization,[36] have recently been introduced. The latter method usually involves in a slurry phase, which requires large volumes of solvents and a need for purification. Thus, this method may be impractical because it is environmentally and economically unfriendly. The melt intercalation of PP–clay nanocomposites usually involves the use of a compatibilizer, such as maleic anhydride grafted polypropylene (PP-*g*-MA), to facilitate the intercalation of PP in clay.[30–32] The maleic anhydride (MA) compatibilizer has mechanical properties lower than those of the native PP, and hence, adding MA compatibilizer can harm the final properties of the composites. Thus, it is necessary to explore the effect of the MA compatibilizer on the final microstructure and properties of the nanocomposites.

In a previous study,[37] we developed a process to help exfoliate and disperse nanoclays into PP matrix with the aid of supercritical CO_2 ($scCO_2$). The process involved the use of a pressurized CO_2 chamber to assist in the exfoliation and delivery of the clay into a stream of polymer melt in the extruder. It was observed that for concentrations as high as 6.6 wt % (only limited by the physical design of the chamber), fairly exfoliated nanocomposites were observed, with as much as a 54% increase in Young's modulus achieved. Most studies dealing with PP–clay nanocomposites, even with the incorporation of a MA compatibilizer, have only been partially successful because complete exfoliation has practically never been reached.[38–52] In this study, the CO_2 chamber technique was extended further by the incorporation of a MA compatibilizer to prepare PP–clay nanocomposites. We wanted to ascertain whether or not further improvements in the mechanical properties of the nanocomposites could be achieved when preparation was done with the incorporation of a MA compatibilizer. The effect of a MA compatibilizer on the microstructure and the mechanical and linear viscoelastic properties of the nanocomposites prepared with two different processing techniques was also studied.

EXPERIMENTAL

Materials

PP (Pro-Fax 6523, melt flow index = 4 g/10 min at 230°C and at a load of 2.16 kg, density = 0.90 g/cm^3) was obtained from Basell (Elkton, MD) and was used as received. PP-*g*-MA (PB3150, melt flow index = 52.2 g/10 min at 230°C and at a load of 2.16 kg, MA content = 0.5 wt %) was supplied from Chemtura Corp. (Middlebury, CT). Surface-modified MMT (Cloisite 20A) was obtained from Southern Clay Products, Inc. (Gonzalez, TX) and was used as received. Cloisite 20A is a surface-modified MMT obtained through a cation-exchange reaction, where the sodium cation is replaced by a dimethyl, dihydrogenated tallow, quaternary ammonium cation.

Clay concentration

Clay concentrations were determined by the burn-off technique in an ashing oven at 500°C for 30 min. The reported concentrations are an average of three burn-off samples. The clay concentrations reported here include the organic modifiers.

Extrusion experiments

Compatibilized PP–clay nanocomposites were prepared by direct-melt compounding and with a modified pressurized CO_2 chamber.[37] Samples were extruded at a melt temperature of around 190°C and a screw speed of 15 rpm with a Killion KL-100 extruder with a single, two-stage screw, 25.4 mm (1 in.) in diameter and with a 30:1 length/diameter ratio (L/D). A capillary die 1/16 in. in diameter and with a 20:1 L/D was attached at the end of the extruder. The chamber was inserted between the CO_2 pump and the injection port at the beginning of the second stage of the screw. A schematic diagram of the overall process is shown in Figure 1.

It was shown in our previous study[37] that the method of direct injection of $scCO_2$ into the barrel during extrusion (METH#2) did not show many property improvements over the conventional direct-melt compounding technique (METH#1) because of its inability to adequately exfoliate and disperse the nanoclay into the polymer matrix. For this reason, METH#2 was not examined again in this study. The two processing methods explored in this study are described next. For each blending technique, an approximate 3:1 ratio of MA compatibilizer to clay was used.

METH#1 + MA (direct melt blending)

METH#1 consisted of conventional single-screw melt compounding. The clay, PP, and PP-*g*-MA were dry

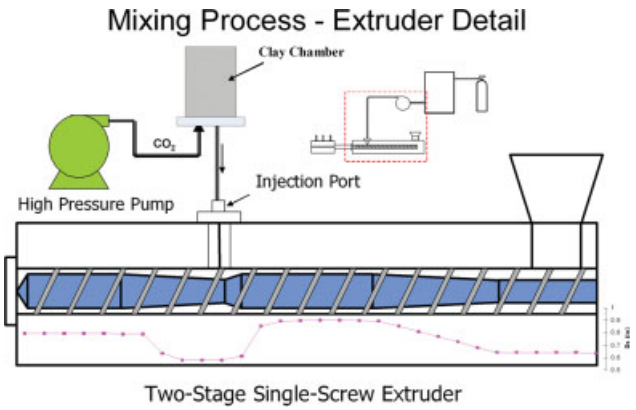

Figure 1 Schematic diagram of the overall process showing the CO_2 chamber and the two-stage single-screw extruder. [Color figure can be viewed in the online issue, which is available at www.interscience.wiley.com.]

blended in a Kitchen Aid type mixer, and then, the mixture was fed to an extruder and repelletized.

METH#3 + MA: CO_2 chamber

The clays were allowed to be in direct contact with $scCO_2$ at 3000 psi and 80°C for a period of time (12–24 h), and then, the pressure was rapidly released. The mixture of the nanoparticles and $scCO_2$ was then injected into the molten polymer stream in a single-screw extruder.

Injection molding

The nanocomposite pellets were dried at 100°C in an oven overnight and then injection-molded with an Arburg Allrounder (model 221-55-250) injection molder. The Arburg Allrounder had a 22-mm diameter barrel, a L/D of 24, a screw with a variable root diameter from approximately 14.25 mm at the feed to 19.3 mm at the exit, a check ring nonreturn valve, and an insulated nozzle that was 2 mm in diameter. The composites were injection-molded with a melt temperature of 200°C, a mold temperature of 80°C, a holding pressure of 5 bars, a screw speed of 200 rpm, and a rectangular endgated mold with dimensions $80 \times 76 \times 1.5$ mm^3.

Rheological properties

Rheological studies of the nanocomposites were performed with a Rheometrics mechanical spectrometer model 800 (RMS-800). Samples were prepared by compression molding of the extruded pellets, which were 25-mm diameter disks. Dynamic frequency sweep experiments were performed under a continuous nitrogen atmosphere with a 25-mm parallel-plate fixture at 200°C in the linear viscoelastic region of the materials. To determine the limits of the linear viscoelastic properties of the materials, dynamic strain sweeps were performed at 200°C and a frequency of 10 rad/s for a filled system with 6.7 wt % Cloisite 20A. The samples were observed to exhibit linear viscoelastic behavior for strains of less than about 8%. The storage, or elastic, modulus (G'), loss modulus (G''), and complex viscosity (η^*) values of the materials as functions of angular frequency (ranging from 0.1 to 100 rad/s) were obtained.

Tensile properties

The injection-molded plaques were cut into rectangular bars, typically along the machine direction, approximately 8.5 mm wide, 1.5 mm thick, and 80 mm long. Tensile tests on these bars were performed at room temperature with an Instron model 4204 testing machine (Instron, Grove City, PA). An extensiometer was used to accurately determine the elongation of the sample and, hence, the Young's modulus and yield strength. The load was measured with a 5-kN load cell, whereas the crosshead speed was kept at 1.27 mm/min during all tensile tests. For all tests, the average and the standard deviation were calculated from at least four samples, and data points greater than 2 standard deviations from the mean were omitted.

Structure and morphological characterization

Wide-angle X-ray diffraction scans were not conducted in this study due to limited access to an X-ray diffraction machine. The processing techniques and conditions were kept the same for this study as they were for the previous study.[37] Therefore, we assumed that the relative trend of the wide-angle X-ray diffraction patterns for the nanocomposites generated in this study were the same as those of the previous study. Transmission electron microscopy (TEM) was used to confirm the morphology of the composites. TEM micrographs were generated with a Philips EM420T with an accelerating voltage of 100 kV. The TEM samples, around 95 nm thick, were cut with a cryomicrotom equipped with a diamond knife at −100°C. Injection-molded samples were used for TEM.

RESULTS AND DISCUSSION

TEM

To qualitatively understand the internal structure of the composites and to examine the degree of dispersion of the clay in the matrix, TEM analysis was carried out. TEM micrographs (at magnifications of 17,000 and 34,000×) of various nanocomposites

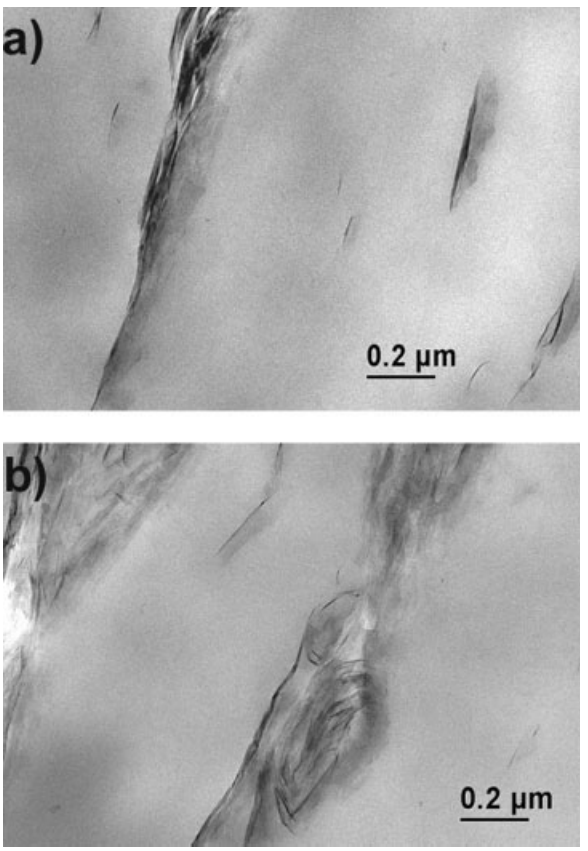

Figure 2 METH#1 4 wt %: (a) 17,000 and (b) 34,000×.

prepared with different processing techniques are presented in Figures 2–5. As shown in Figure 2, the 4 wt % nanocomposite prepared via METH#1 without the MA compatibilizer showed very poor dispersion. Mostly, an intercalated structure with very large aggregates or tactoids in the order of several tens to hundreds of silicate layers was observed. This observation is common because of the lack of the affinity between the polar clay and the highly nonpolar polymer matrix. With the same processing method plus the incorporation of PP-*g*-MA, better dispersion was observed (Fig. 3). Clearly, the size of the aggregates was greatly reduced, although some aggregates still existed. It is apparent from this observation that the MA compatibilizer had a positive effect on the dispersion of the clay into the PP matrix. The ability of the polar functional groups to hydrogen bond and interact with the silicate surface helped promote diffusion of the polymer chains into the clay galleries. Further improvement in the exfoliation of the clay particles in the PP matrix was observed when PP-*g*-MA was used in METH#3 (Figs. 4 and 5). As shown in the TEM micrographs in Figures 4 and 5, the nanocomposite was fairly well dispersed and the clay was evenly distributed throughout the polymer matrix. Although there were still some areas that showed thick silicate layers, most showed fairly well-dispersed clay platelets, even at high magnification. This observation was consistent with that of the previous study, which further confirmed the effectiveness of METH#3 in dispersing the silicate into the polymer matrix.

Tensile properties

In the previous study,[37] we reported the mechanical properties of various PP–clay nanocomposites prepared without the incorporation of a MA compatibilizer with different processing techniques. In general, we found that the conventional direct-melt compounding methods (METH#1 and METH#2) with single-screw extrusion, with and without the direct injection of $scCO_2$, did not lead to much improvement in the mechanical properties of the injection-molded samples because of their inability to adequately exfoliate the nanoparticles into the polymer matrix. However, most improvements were seen from the technique that used the pressurized CO_2 chamber (METH#3). As much as a 54% increase in Young's modulus was obtained for 6.6 wt % clay.

In this section, the effect of a MA compatibilizer on the mechanical performance of the nanocomposites prepared with the two different processing techniques described previously (METH#1 and #3) is

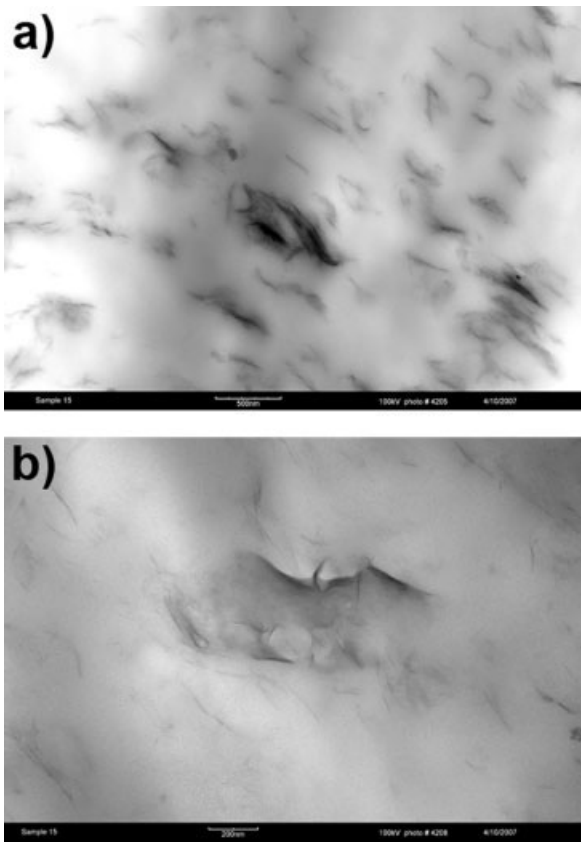

Figure 3 METH#1 + MA 4.3 wt %: (a) 17,000 and (b) 34,000×.

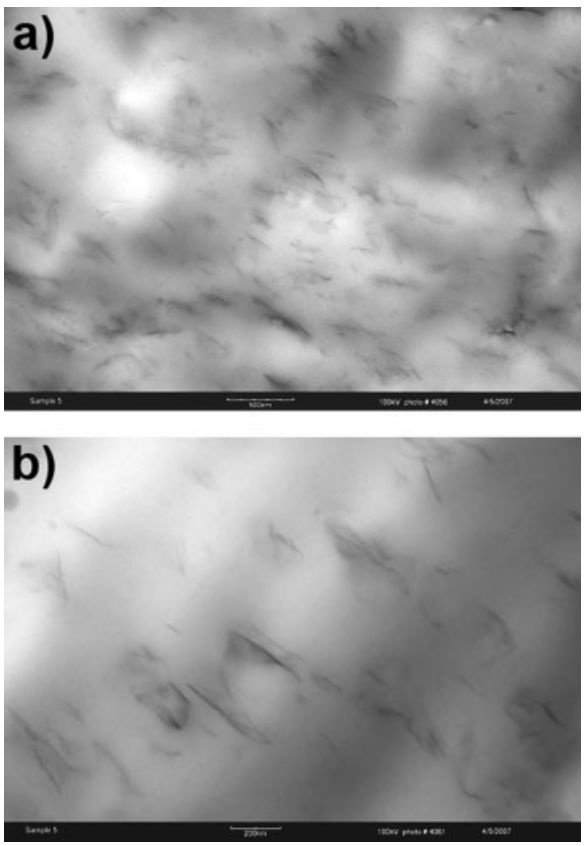

Figure 4 METH#3 + MA 4.2 wt %: (a) 17,000 and (b) 34,000×.

examined. The tensile properties presented in the following discussion are summarized in Table I and Figure 6. In Figure 6, the mechanical properties of the noncompatibilized PP–clay nanocomposites obtained from the previous study for METH#1 and METH#3 are also plotted for comparison. Analyzing the trends of the mechanical properties could give useful information about the effect of the MA compatibilizer and processing methods on the nanocomposites' performance. Comparing the mechanical properties of the compatibilized and noncompatibilized nanocomposites prepared via METH#1, we saw that the mechanical properties of the compatibilized nanocomposites were much more enhanced than those of the noncompatibilized ones at all clay levels. As much as a 20% additional increase in Young's moduli and a 15–20% additional increase in the yield strengths were observed for the compatibilized composites. It is important to point out, however, that the mechanical properties of the compatibilized composites prepared via METH#1 also showed little increase beyond the addition of 4.0 wt %, which is a common observation.[53–55] When METH#3 was used with the incorporation of MA compatibilizer, further improvements in the mechanical properties were achieved at all clay levels. At clay loading of 6.8 wt %, as much as a 69% increase in Young's modulus and a 13% increase in yield strength were observed. In both processing methods, the addition of MA compatibilizer greatly enhanced the mechanical performance of the nanocomposites. This was due to the compatibilizer that was used in preparation of the nanocomposite, which increased the bonding between the nanoparticles and the PP matrix and helped with dispersion. Despite the improvements in the yield strength and Young's modulus, we observed a decrease in the elongation at break values with increasing clay content for the compatibilized PP–clay nanocomposites. In this kind of system, this behavior is common because the clay can act as a defect and affect the deformation capability.[56]

Comparing the tensile properties of the compatibilized nanocomposites prepared with METH#1 to those of the noncompatibilized nanocomposites prepared with METH#3, we observed that those prepared with METH#3, even without a MA compatibilizer, could still perform as well as those prepared with METH#1 with a MA compatibilizer. Also, the noncompatibilized composites prepared via METH#3 possessed much higher elongation at break values than those of the compatibilized composites prepared via METH#1 at all clay levels. This, again, proves that METH#3 was much more effective than

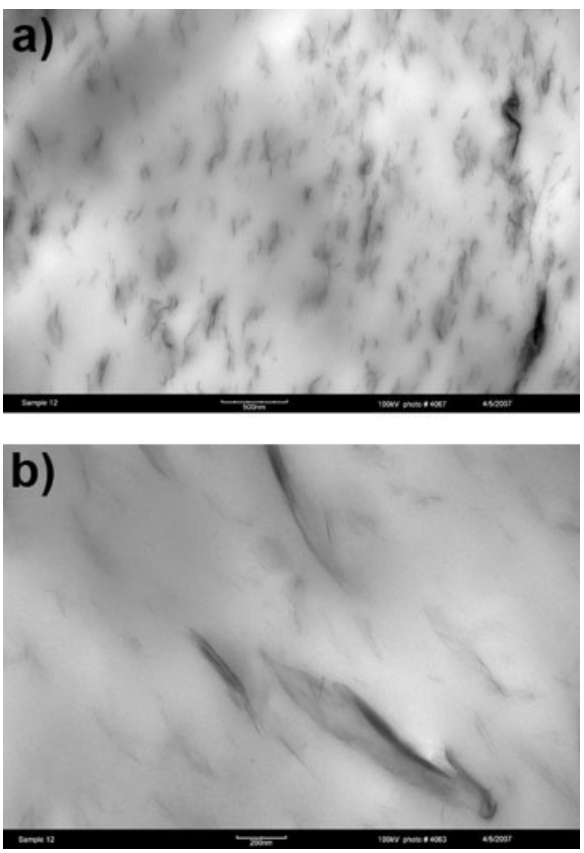

Figure 5 METH#3 + MA 6.8 wt %: (a) 17,000 and (b) 34,000×.

TABLE I
Tensile Properties of Various Nanocomposites Prepared with Different Processing Methods

Material	Young's modulus (GPa)	SD	% increase	Yield strength (MPa)	SD	% elongation	SD
Pure PP	1.374	0.133	—	15.16	0.47	115.3	19.79
METH#1 + MA 4.3 wt %	1.916	0.023	39	16.68	0.38	17.06	13.21
METH#1 + MA 6.7 wt %	2.073	0.076	51	18.21	0.64	11.62	4.75
METH#1 + MA 12 wt %	2.158	0.195	57	15.84	0.84	17.78	10.31
METH#3 + MA 4.2 wt %	2.020	0.134	47	17.15	0.47	16.23	4.92
METH#3 + MA 6.8 wt %	2.326	0.093	69	17.03	0.24	7.13	2.30

SD = standard deviation.

METH#1 in terms of its ability to better disperse the nanoclay into the polymer matrix to achieve better mechanical properties. Additionally, as shown in the mechanical response curves in Figure 6, the nanocomposites prepared via METH#3 could potentially exhibit higher mechanical properties beyond a clay level of 6.7 wt % (if not limited by these process capabilities), whereas in METH#1, even with the incorporation of a MA compatibilizer, the mechanical properties leveled out beyond a clay level of 4 wt %.

To realize the full potential of the mechanical property increase, it is necessary to compare the observed property enhancements, such as modulus, to those predicted by composite theories, such as that of Halpin-Tsai.[57,58] Halpin-Tsai's model, shown in eq. (1), assumes fully exfoliated clay platelets; unidirectional, that is, well-oriented, filler particles; and a high degree of adhesion of the filler particles to the surrounding polymer matrix:

$$E_c = E_m \left[\frac{1 + \zeta \eta \phi_f}{1 - \eta \phi_f} \right] \tag{1}$$

where E_c is the composite modulus, E_m is the unfilled matrix modulus, ζ is used to describe the influence of geometry of the reinforcing phase, and ϕ_f is the filler volume fraction:

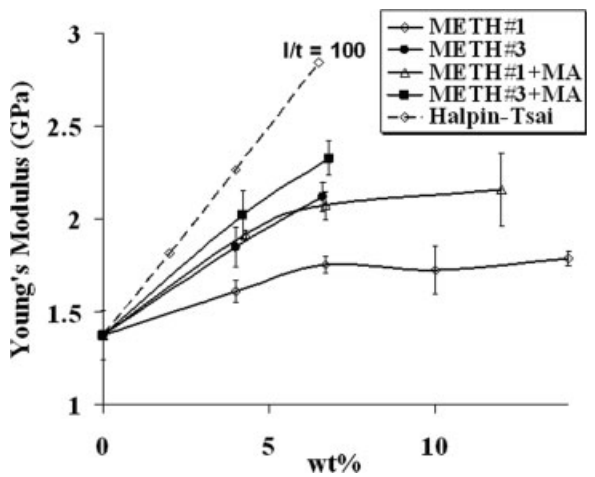

Figure 6 Young's modulus of different nanocomposites prepared with different processing techniques.

$$\eta = \frac{E_f/E_m - 1}{E_f/E_m + \zeta} \tag{2}$$

$$\zeta = 2(l/t) \tag{3}$$

where E_f is the filler modulus, which was taken to be 178 GPa for MMT,[58] and l/t is the aspect ratio of the silicate platelets, which was taken here to be approximately 100 for fully exfoliated platelets.[58]

The theoretical and experimentally measured moduli of the composites versus the weight percentage of MMT is shown in Figure 6. As shown, the experimental Young's moduli presented were below those predicted by the Halpin-Tsai model. Although the values were closer for the compatibilized nanocomposites, they were still below those of the theory prediction. The difference must be attributed to the assumptions made in the Halpin-Tsai theory. It is important to point out that there numerous complexities arise when one compares experimental data to those of composite theory, especially when dealing with polymer layered-silicate nanocomposites. The main reasons for the difference may have been due to a lack of complete orientation of the filler particles in the flow direction or imperfect bonding between the filler and the matrix or the aspect ratio of the platelets may have been much less than the assumed value of 100.

Linear viscoelastic properties

In this section, we look at the effect of the MA compatibilizer on the rheological behavior of the nanocomposite melts prepared with different processing techniques at various levels of nanoclay. G', G'', and η^* values resulting from the dynamic frequency scan measurements are compared in Figures 7, 8, and 9, respectively. The results from the previous study[37] for processing METH#3 without the incorporation of a MA compatibilizer are also shown in these figures for comparison.

According to our previous study,[37] the nanocomposites prepared by METH#3 did not exhibit a tail or plateau in G' at low frequencies, even though a good degree of clay dispersion was observed by

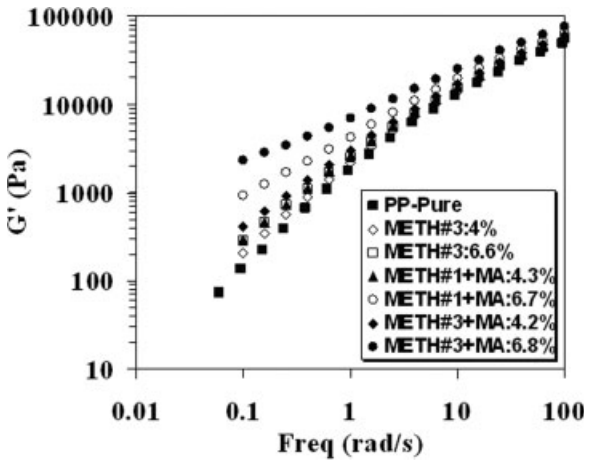

Figure 7 G' versus frequency (Freq.) of different nanocomposites at 200°C.

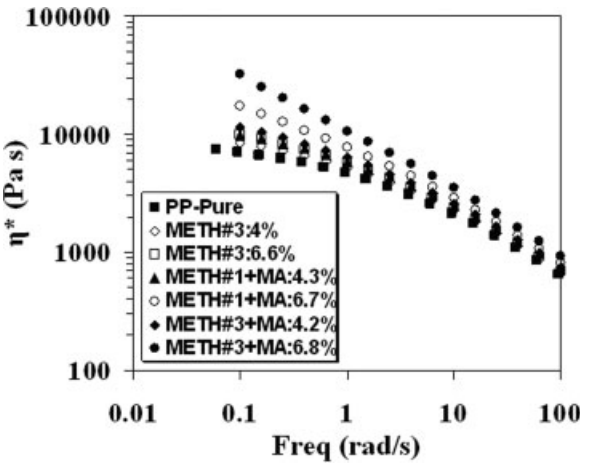

Figure 9 η* versus frequency (Freq.) of different nanocomposites at 200°C.

X-ray diffraction and TEM. However, moderate enhancement in G' at low frequencies was noticed, which we hypothesized to arise from the interactions between the exfoliated clay platelets. Here, the lack of a tail in G', as we mentioned in the previous article, could have been due to the absence of a network formed by the strong hydrogen bonding between the polar functional groups of PP-*g*-MA and the hydroxyl groups of the silicate.

In this study, we clearly observed the onset plateaus of G' and G'' (Figs. 7 and 8) and the diverging of η* (Fig. 9) at low frequencies for all of the nanocomposites prepared with the incorporation of MA compatibilizer with METH#1 and METH#3. A direct comparison of the rheological response of the nanocomposites prepared with and without the use of PP-*g*-MA showed a direct effect of the MA compatibilizer on the enhancement of low-frequency G', G'', and η*. The reason for the increase in G', G'', and η* could be the use of a MA compatibilizer, which increased the interaction and hydrogen bonding between the filler and polymer matrix, which probably led to a lower polymeric chain mobility and made the material more rigid and solidlike. Many researchers believe that the pseudosolidlike behavior at low frequencies might be ascribed to the formation of a percolated network structure of the clay platelets or the frictional interactions between the anisotropic clay tactoids.[59–63] Comparing the low-frequency G' of the compatibilized PP–clay nanocomposites prepared via METH#1 and METH#3, we observed that the low-frequency G' of the composites prepared with METH#3 was more enhanced at both clay levels of 4.3 and 6.7 wt %. If we assume that everything else was constant except for the processing technique, the increase in the low-frequency G' must have been due to the increased particle–particle interactions due to better dispersion, which resulted from the pressurized CO_2 chamber technique. Also, when the layered-silicate particles were more exfoliated, there would have been more surface area available for the MA groups to hydrogen bond with the hydroxyl groups on the clay surface to form a network. This increase in network formation could have contributed to the increase in G' at low frequencies.

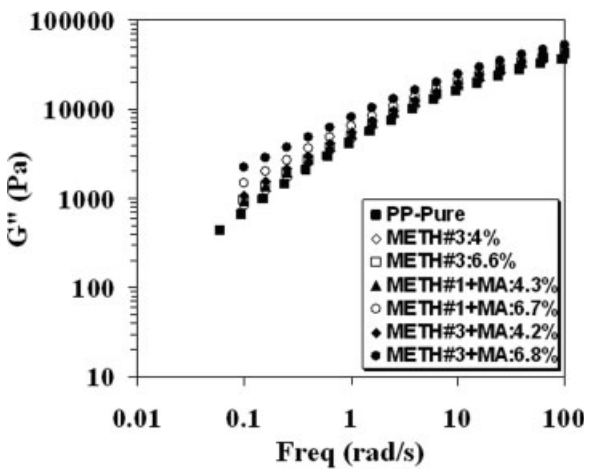

Figure 8 G'' versus frequency (Freq.) of different nanocomposites at 200°C.

The use of rheology to determine the degree of exfoliation of the nanocomposites is still ambiguous, and the information obtained from it can only be used to probe the structure of the layered silicate indirectly. It still remains unclear in the literature whether the changes in dynamic rheological properties in the low-frequency region were due to the interactions of exfoliated clay platelets within the maleated PP matrix or whether a network occurred between the MA groups and the hydroxylated surfaces of the silicate layers.[64,65] The results presented in this article lead us to believe that the enhancement of the low-frequency G' was a contribution of both

the interparticle interaction and the polymer–clay interaction. Thus, the rheological properties commonly reported for clay-filled functionalized PP cannot be attributed solely to the formation of a percolation network between clay platelets, but the contribution and the properties of the functionalized matrix must be considered.

CONCLUSIONS

Compatibilized PP–clay nanocomposites were prepared in this study via direct melt intercalation and with the pressurized CO_2 chamber technique. The degree of dispersion and the mechanical and rheological properties of the nanocomposites were greatly affected by the incorporation of a MA compatibilizer. The polarity and reactivity of the functional groups of MA helped to improve the interaction between the filler and polymer, which led to better dispersion of the silicate platelets, an enhanced G' at low frequencies, and improved mechanical performance. The greatest improvements were seen with the technique that used the pressurized CO_2 chamber with the incorporation of PP-*g*-MA. TEM data showed a fairly good degree of exfoliation for concentrations as high as 6.8 wt %, and the mechanical properties, such as modulus, increased by as much as 69% relative to that of PP matrix.

The authors thank Chemtura Corp. for providing PP-*g*-MA and Steve McCartney at the Virginia Polytechnic Institute and State University Materials Research Institute for aid in conducting the TEM study.

References

1. Usuki, A.; Kojima, Y.; Kawasumi, M.; Okada, A.; Fukushima, Y.; Kurauchi, T.; Kamigaito, O. J Mater Res 1993, 8, 1185.
2. Kojima, Y.; Usuki, A.; Kawasumi, M.; Okada, A.; Kurauchi, T.; Kamigaito, O. J Polym Sci Part A: Polym Chem 1993, 31, 983.
3. Kojima, Y.; Usuki, A.; Kawasumi, M.; Okada, A.; Kurauchi, T.; Kamigaito, O. J Polym Sci Part A: Polym Chem 1993, 31, 1755.
4. Liu, L.; Qi, Z.; Zhu, X. J Appl Polym Sci 1999, 71, 1133.
5. Lan, T.; Kaviratna, D.; Pinnavaia, T. J. Chem Mater 1994, 6, 573.
6. Gilman, W.; Morgan, A.; Giannelis, P.; Wuthenow, M.; Manias, E. In Flame Retardancy 10th Annual BBC Conference Proceedings, 1999; p 1.
7. Giannelis, P. Appl Organomet Chem 1998, 12, 675.
8. Okada, A.; Kawasumi, M.; Usuki, A.; Kojima, Y.; Kurauchi, T.; Kamigaito, O. In Polymer Based Molecular Composites MRS Symposium Proceedings, Pittsburgh, 1990; Schaefer, W.; Mark, E., Ed.; Vol. 171, p 45.
9. Giannelis, P. Adv Mater 1996, 8, 29.
10. Giannelis, E. P.; Krishnamoorti, R.; Manias, E. Adv Polym Sci 1999, 138, 107.
11. LeBaron, P. C.; Wang, Z.; Pinnavaia, T. J. Appl Clay Sci 1999, 15, 11.
12. Vaia, R. A.; Price, G.; Ruth, P. N.; Nguyen, H. T.; Lichtenhan J. D. Appl Clay Sci 1999, 15, 67.
13. Biswas, M.; Sinha, S. Adv Polym Sci 2001, 55, 167.
14. Gilman, J. W. Appl Clay Sci 1999, 15, 31.
15. Bins & Associates. Plast Additives Compd 2002, 4, 30.
16. Lan, T.; Kaviratna, P. D.; Pinnavaia, T. J. Chem Mater 1994, 6, 573.
17. Sall, K. Eur Plast News 2002, March 14.
18. Messersmith, P. B.; Giannelis, E. P. J Polym Sci Part A: Polym Chem 1995, 33, 1005.
19. Gilman, J. W.; Kashiwagi, T.; Lichtenhan, J. D. SAMPE J 1997, 33, 40.
20. Gilman, J. W. Appl Clay Sci 1999, 15, 31.
21. Dabrowski, F.; Bras, L.; Bourbigot, S.; Gilman, J. W.; Kashiwagi, T. In Proceedings of the Eurofillers, Lyon-Villeurbanne, France, 1999; pp 6, 9.
22. Bourbigot, S.; LeBras, M.; Dabrowski, F.; Gilman, J. W.; Kashiwagi, T. Fire Mater 2000, 24, 201.
23. Gilman, J. W.; Jackson, C. L.; Morgan, A. B.; Harris, R.; Manias, E.; Giannelis, E. P.; Wuthenow, M.; Hilton, D.; Phillips, H. Chem Mater 2000, 12, 1866.
24. Mehrabzadeh, M.; Kamal, M. R. Polym Eng Sci 2004, 44, 152.
25. Pinnavaia, T. J.; Beall, G. W. Polymer–Clay Nanocomposites; Wiley: New York, 2000.
26. Zanetti, M.; Lomakin, S.; Camino, G. Macromol Mater Eng 2000, 279, 1.
27. Blumstein, A. J Polym Sci Part A: Gen Pap 1965, 3, 2665.
28. Theng, B. K. G. Formation and Properties of Clay–Polymer Complexes; Elsevier: Amsterdam, 1979.
29. Krishnamoorti, R.; Vaia, A.; Giannelis P. Chem Mater 1996, 8, 1728.
30. Kawasami, M.; Hasegawa, N.; Kato, M.; Usuki, A.; Okada, A. Macromolecules 1997, 30, 6333.
31. Nam, P. H.; Maiti, P.; Okamoto, M.; Kotaka, T.; Hasegawa, N.; Usuki, A. Polymer 2001, 42, 9633.
32. Kato, M.; Usuki, A.; Okada, A. J Appl Polym Sci 1997, 66, 1781.
33. Modesti, M.; Lorenzetti, A.; Bon, D.; Besco, S. Polymer 2005, 46, 10237.
34. Kanny, K.; Moodley, V. K. J Eng Mater Tech 2007, 129, 105.
35. Lee, J. W.; Kim, M. H.; Choi, W. M.; Park, O. O. J Appl Polym Sci 2006, 99, 1752.
36. Alexandre, M.; Dubois, P. Mater Sci Eng 2000, 28, 1.
37. Nguyen, Q. T.; Baird, D. G. Ph.D. Dissertation, Virginia Polytechnic Institute and State University, 2007.
38. Modesti, M.; Lorenzetti, A.; Bon, D.; Besco, S. Polymer 2005, 46, 10237.
39. Kanny, K.; Moodley, V. K. J. Eng Mater Tech 2007, 129, 105.
40. Lee, J. W.; Kim, M. H.; Choi, W. M.; Park, O. O. J Appl Polym Sci 2006, 99, 1752.
41. Alexandre, M.; Dubois, P. Mater Sci Eng 2000, 28, 1.
42. Ray, S. S.; Okamoto, M. Prog Polym Sci 2003, 28, 1539.
43. Pinnavaia, T. J.; Beall, G. W. Polymer–Clay Nanocomposites; Wiley: New York, 2000.
44. LeBaron, P. C.; Wang, Z.; Pinnavaia, T. J. Appl Clay Sci 1999, 15, 11.
45. Fornes, T. D.; Paul, D. R. Polymer 2003, 44, 4993.
46. Osman, M. A.; Rupp, J. E. P.; Suter, U. W. Polymer 2005, 46, 1653.
47. Wang, Z. M.; Nakajima, H.; Manias, E.; Chung, T. C. Macromolecules 2003, 36, 8919.
48. Manias, E. In Origins of the Materials Properties Enhancements in Polymer/Clay Nanocomposites; Golovoy, A., Ed.; Nanocomposites 2001, Delivering New Value to Plastics; ECM: Chicago, 2001.
49. Dennis, H. R.; Hunter, D. L.; Chang, D.; Kim, S.; White, J. L.; Cho, J. W.; Paul, D. R. Polymer 2001, 42, 9513.
50. Manias, E.; Touny, A.; Wu, L.; Strawhecker, K.; Lu, B.; Chung, T. C. Chem Mater 2001, 13, 3516.
51. Svoboda, P.; Zeng, C. C.; Wang, H.; Lee, L. J.; Tomasko, D. L. J Appl Polym Sci 2002, 85, 1562.

52. Ellis, T. S.; D'Angelo, J. S. J Appl Polym Sci 2003, 90, 1639.
53. Hasegawa, N.; Okamoto, H.; Kawasumi, M.; Kato, M.; Tsukigase, A.; Usuki, A. Macromol Mater Eng 2000, 280, 76.
54. Reichert, P.; Nitz, H.; Klinke, S.; Brandsch, R.; Thomann, R.; Mülhaupt, R. Macromol Mater Eng 2000, 275, 8.
55. Kim, K. N.; Kim, H.; Lee, J. W. Polym Eng Sci 2001, 41, 1963.
56. Lopez-Quintanilla, M. L.; Sanchez-Valdes, S.; Ramos de Valle, L. F.; Medellin-Rodriguez, F. J. J Appl Polym Sci 2006, 100, 4748.
57. Halpin, J. C.; Kardos, J. L. Polym Eng Sci 1976, 16, 344.
58. Fornes, T. D.; Paul, D. R. Polymer 2003, 44, 4993.
59. Ren, J.; Casanueva, B. F.; Mitchell, C. A.; Krishamoorti, R. Macromolecules 2003, 36, 4188.
60. Krishnamoorti, R.; Yurekli, K. Curr Opin Colloid Interface Sci 2001, 6, 464.
61. Galgali, G.; Ramesh, C.; Lele, A. Macromolecules 2001, 34, 852.
62. Solomon, M. J.; Almuallam, A. S.; Seefeldt, K. F.; Somwangth-Anaroj, A.; Varadan, P. Macromolecules 2001, 34, 1864.
63. Litchfield, D. W.; Baird, D. G. Rheol Rev 2006, 1.
64. Gilman, J. W.; Jackson, C. L.; Morgan, A. B.; Harris, R., Jr. Chem Mater 2000, 12, 1807.
65. Lee, J. A.; Kontopoulou, M.; Parent, J. S. Polymer 2004, 45, 6595.